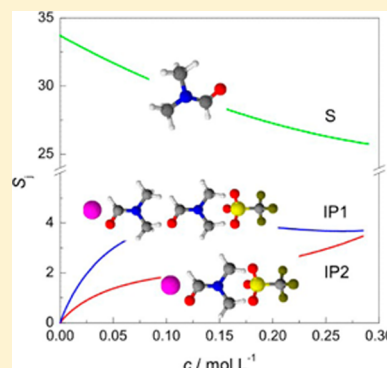


# Solvation and Association of 3:1 Electrolytes in *N,N*-Dimethylformamide

Anna Fuchs,<sup>†,‡,#</sup> Richard Buchner,<sup>\*,‡</sup> and Glenn Heffer<sup>\*,†</sup><sup>†</sup>Chemistry Department, Murdoch University, Murdoch, Western Australia 6150, Australia<sup>‡</sup>Institut für Physikalische und Theoretische Chemie, Universität Regensburg, D-93040 Regensburg, Germany

## S Supporting Information

**ABSTRACT:** A detailed study has been made of the solvation and ion association of the trifluoromethanesulfonate ( $\text{TF}^-$ ) salts of aluminum(III), scandium(III), and lanthanum(III) in *N,N*-dimethylformamide (DMF) at 25 °C using dielectric relaxation spectroscopy over the frequency range of  $0.1 \lesssim \nu/\text{GHz} \lesssim 89$ . The spectra of all solutions exhibited either two (for  $\text{ScTF}_3$  and  $\text{LaTF}_3$ ) or three (for  $\text{AlTF}_3$ ) relaxation processes, a dominant mode centered at  $\sim 15$  GHz due to the solvent and one or (for  $\text{AlTF}_3$  solutions) two solute-related processes at lower frequencies ( $\nu_{\text{max}} \lesssim 2$  GHz). Effective solvation numbers,  $Z_{\text{ib}}$ , calculated from the solvent relaxation process indicated that all three cations were strongly solvated by DMF with  $Z_{\text{ib}}^0$  values at infinite dilution in the order ( $\text{Al}^{3+} \approx \text{Sc}^{3+} \approx 10$ ) < ( $\text{La}^{3+} \approx 13$ ), consistent with at least partial formation of a second solvation shell around each cation. One solute-related mode for each set of salt solutions was assigned to the rotational diffusion of solvent-shared ion pairs (SIPs) of 1:1 stoichiometry; the additional slower process for  $\text{AlTF}_3$  solutions in DMF was attributed to the presence of double-solvent-separated IPs. The overall association constants at infinite dilution for the 1:1 IPs,  $K_A^\circ(\text{MTF}^{2+})$ , were significant, but as expected from Debye–Hückel considerations, the  $K_A$  values decreased rapidly with increasing solute concentration.



## 1. INTRODUCTION

The solvation and association of ions governs virtually all of the observable characteristics of electrolyte solutions, including their physical properties (conductivity, heat capacity, etc.) and their chemical behavior such as their acidity/basicity, redox activity, complexing tendency, solubility, and kinetics.<sup>1,2</sup> The great variation in behavior that can occur when electrolytes are dissolved in different solvents is the rationale for the ongoing interest in the investigation of the properties of nonaqueous electrolyte solutions, including ionic liquids.<sup>3</sup> Such diversity offers wide prospects for technological innovation, although in practice there are always many difficulties to be overcome.<sup>3</sup>

Just a cursory glance at the literature reveals that almost all studies of nonaqueous electrolyte solutions to date have focused on a rather narrow range of 1:1 salts. For some properties, even *qualitative* descriptions of the effects of ion charge are not (or at best are barely) possible. For example, in their comprehensive review of electrolyte volumes, Marcus and Heffer noted that there were almost no reliable volumetric data in any nonaqueous solvent for non-1:1 electrolytes.<sup>4</sup> Even for relatively easily measured properties such as Gibbs energies<sup>5</sup> and viscosities,<sup>6</sup> there are very few data available for highly charged electrolytes, making meaningful comparisons with theoretical predictions or computer simulations almost impossible. Electrical conductivities<sup>7</sup> are a partial exception to this dismal scene, but the database for polyvalent electrolytes in nonaqueous solvents is hardly comprehensive or satisfactory.<sup>7</sup>

There is therefore a need for investigations that characterize the behavior of multivalent electrolytes in nonaqueous solvents.

Among the many techniques available for studying ion solvation and ion association in solution, dielectric relaxation spectroscopy (DRS) has a number of advantages.<sup>8,9</sup> These include its ability to quantify ion solvation in a straightforward manner, its sensitivity toward ion pairs (IPs), especially solvent-separated IPs that are hard to detect using other techniques, and its ready applicability to virtually all solvents and salt types, including non-1:1 and asymmetric electrolytes.

The present work reports the dielectric spectra of three 3:1 electrolytes, the trifluoromethanesulfonate (triflate,  $\text{TF}^-$ ,  $\text{CF}_3\text{SO}_3^-$ ) salts of aluminum(III), scandium(III), and lanthanum(III) in the nonaqueous solvent *N,N*-dimethylformamide (DMF). To the best of our knowledge, these are the first DRS measurements reported for any 3:1 salt in any solvent other than water, and even in the latter, such investigations are rather few.<sup>10</sup> The cations were selected on the basis of their significantly differing radii,<sup>11</sup> while the triflate ion was used to provide sufficiently soluble salts and because its delocalized charge usually means that it shows minimal interaction (ion pairing) with cations. DMF was chosen as the solvent because of the ready availability of subsidiary information<sup>12,13</sup> to assist in the interpretation of the results, including previous DRS

Received: September 6, 2013

Revised: October 29, 2013

Published: October 30, 2013

studies of 1:1 and 2:1 salts.<sup>14,15</sup> Such solutions are also of interest because DMF is widely employed in chromatography<sup>16</sup> and is a useful solvent for a wide variety of inorganic and organic substances, including polymers and paints.

## 2. EXPERIMENTAL SECTION

**2.1. Reagents.** Triflate salts of  $\text{Sc}^{3+}$  and  $\text{La}^{3+}$  were prepared respectively by neutralization of suspensions of  $\text{Sc}_2\text{O}_3(\text{s})$  and  $\text{La}_2\text{O}_3(\text{s})$  in AR methanol by dropwise addition of “triflic” acid ( $\text{CF}_3\text{SO}_3\text{H}$ ; HTF; 3M Company, U.S.A., AR grade). The crude salts so obtained were collected, purified, and dried as described elsewhere.<sup>13</sup> Aluminum triflate,  $\text{Al}(\text{CF}_3\text{SO}_3)_3$ , was obtained from Sigma–Aldrich (U.S.A., LR grade) and was dried under vacuum at room temperature for 24 h. Solvent DMF (Merck, Germany, AR grade, 99.5%) was dried and stored over freshly activated 3 Å molecular sieves and typically had a water content (coulometric Karl Fischer titration) of <200 ppm. Solutions were prepared by weight in a drybox, without buoyancy corrections, using syringe techniques. Density data required for the conversion of concentrations to the  $\text{mol L}^{-1}$  scale were those reported previously.<sup>13</sup>

**2.2. Measurements.** Dielectric spectra over the frequency range of  $0.2 \leq \nu/\text{GHz} \leq 89$  were recorded using three instruments, a Hewlett–Packard 8720D vector network analyzer (VNA) with a HP 85070 dielectric probe kit, covering the range of  $0.2 \leq \nu/\text{GHz} \leq 20$ , at Murdoch University and two waveguide interferometers operating at  $27 \leq \nu/\text{GHz} \leq 89$  at Regensburg University.<sup>17,18</sup> Some additional measurements up to 50 GHz were made at Regensburg using an Agilent E8364B VNA with two Agilent probes (85070-020 and -050). Both VNAs were calibrated using air, mercury, and dried AR grade *N,N*-dimethylacetamide; the interferometers do not require calibration. All measurements were made in at least duplicate at  $(25 \pm 0.02)^\circ\text{C}$ , with a NIST-traceable temperature accuracy of  $\pm 0.05^\circ\text{C}$ . Further details on the measurement procedures have been given previously.<sup>17,18</sup> The required electrical conductivities,  $\kappa$ , were measured at low frequencies ( $\nu < 2$  kHz), as described elsewhere.<sup>15</sup>

**2.3. Data Analysis.** The experimentally accessible quantity in dielectric spectroscopy is the total complex permittivity,  $\eta^*(\nu)$ , which is measured as a function of the frequency,  $\nu$ , of the applied electric field<sup>8,9</sup>

$$\eta^*(\nu) = \eta'(\nu) - i\eta''(\nu) \quad (1)$$

The desired dielectric quantities are the relative permittivity,  $\epsilon'(\nu) = \eta'(\nu)$ , and the dielectric loss

$$\epsilon''(\nu) = \eta''(\nu) - \frac{\kappa}{(2\pi\nu\epsilon_0)} \quad (2)$$

where  $\kappa$  is the dc electrical conductivity of the sample and  $\epsilon_0$  is the electrical permittivity of free space. Although  $\kappa$  can be measured separately (see above), due to field imperfections of the VNA probe heads, it is better in practice to treat it as an adjustable parameter in the fitting process.<sup>19</sup> Accordingly, experimental  $\kappa$  values were taken as starting approximations at each concentration, and spectra were rejected if the fitted  $\kappa$  values differed by more than 5% from the experimental ones. The conductivities so obtained were subtracted from the observed  $\eta''(\nu)$  values to give (eq 2) the desired conductivity-corrected  $\epsilon''(\nu)$  spectra, which were used for all subsequent calculations.

Following combination of the VNA and interferometer data, the conductivity-corrected dielectric spectra

$$\epsilon^*(\nu) = \epsilon'(\nu) - i\epsilon''(\nu) \quad (3)$$

were fitted with plausible models based on  $n$  individual relaxation processes

$$\epsilon^*(\nu) = \sum_{j=1}^n \frac{\epsilon_j - \epsilon_{j+1}}{[1 + (i2\pi\nu\tau_j)^{1-\alpha_j}]^{\beta_j}} + \epsilon_\infty \quad (4)$$

with each dispersion step  $j$ , of amplitude  $S_j = \epsilon_j - \epsilon_{j+1}$  and relaxation time  $\tau_j$ , being modeled by either a Havriliak–Negami (HN) equation, with relaxation time distribution parameters of  $0 \leq \alpha_j < 1$  and  $0 < \beta_j \leq 1$ , or any of its simplified variants, the Debye (D;  $\alpha_j = 0, \beta_j = 1$ ), Cole–Cole (CC;  $\beta_j = 1$ ), or Cole–Davidson (CD;  $\alpha_j = 0$ ) models. The static (relative) permittivity of the sample is defined as  $\epsilon = \epsilon_\infty + \sum S_j$ , where  $\epsilon_\infty = \epsilon_{n+1} = \lim_{\nu \rightarrow \infty} \epsilon'(\nu)$  is the so-called infinite frequency permittivity. The model chosen was that which gave the lowest value of the reduced error function ( $\chi^2$ ) and relaxation amplitudes and times that were physically realistic and varied smoothly with solute concentration.<sup>20</sup> In addition, randomly selected spectra were analyzed using the procedure of Zaslavsky and Buchner,<sup>21</sup> which provides an unbiased determination of the number and location of D relaxation processes that would be required for formal description of  $\epsilon^*(\nu)$ .

## 3. RESULTS AND DISCUSSION

**3.1. Assignment of Modes.** Typical experimental spectra obtained for the present electrolyte solutions in DMF are shown in Figure 1 for  $\text{Al}(\text{CF}_3\text{SO}_3)_3$ . The corresponding results

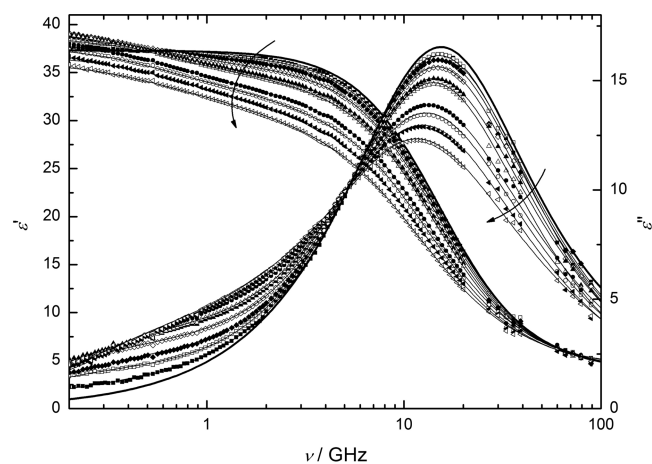


**Figure 1.** Relative permittivity,  $\epsilon'(\nu)$ , and dielectric loss,  $\epsilon''(\nu)$ , spectra of neat DMF and solutions of  $\text{Al}(\text{CF}_3\text{SO}_3)_3$  at  $0.0093 \leq c/\text{mol L}^{-1} \leq 0.2715$  in DMF at  $25^\circ\text{C}$ . The curved arrows indicate increasing  $c$  (Table 1). Lines are fits using a D + D + CD model; heavy lines indicate the neat DMF spectra.

for  $\text{Sc}(\text{CF}_3\text{SO}_3)_3$  and  $\text{La}(\text{CF}_3\text{SO}_3)_3$  solutions are given in the Supporting Information (Figures S1 and S2). Values of the parameters obtained by application of eq 4 to the corrected spectra, along with other relevant information, are given in Table 1 and are further discussed below. As would be expected, given its rather large permanent dipole moment ( $\mu_{\text{DMF}} = 3.86$  D),<sup>12</sup> the DR spectra of all of the present electrolyte solutions are dominated by a large-amplitude process centered at  $\sim 15$  GHz (Figure 1 and Supporting Information Figures S1 and S2), which arises from the rotational diffusion of the solvent molecules and is described by the parameters  $S_j$ ,  $\tau_j$ , and  $\beta_j$  of

**Table 1.** Densities, Conductivities, and Fitting Parameters (D + D + CD and D + CD Models) of the DR Spectra for DMF Solutions of  $\text{Al}(\text{CF}_3\text{SO}_3)_3$ ,  $\text{Sc}(\text{CF}_3\text{SO}_3)_3$ , and  $\text{La}(\text{CF}_3\text{SO}_3)_3$  at 25 °C<sup>a</sup>

$c$	$\rho$	$\kappa$	$\epsilon$	$S_{\text{IP1}}$	$\tau_{\text{IP1}}$	$S_{\text{IP2}}$	$\tau_{\text{IP2}}$	$S_{\text{S}}$	$\tau_{\text{S}}$	$\beta$	$\epsilon_{\infty}$	$10^3 \chi^2$
$\text{Al}(\text{CF}_3\text{SO}_3)_3$												
0	0.943748 <sup>b</sup>	0.0	37.31					34.29	10.42	—	3.02	—
0.0093	0.946516	0.110	37.99	0.90	578	0.22	197	32.63	10.61	0.981	4.23	3.3
0.0162	0.948667	0.175	39.07	1.59	664	0.73	281	33.11	11.05	0.938	3.65	7.9
0.0267	0.951653	0.260	39.26	2.53	425	0.46	162	32.63	11.15	0.938	3.64	12.2
0.0456	0.957157	0.402	40.00	2.84	526	1.60	172	31.76	11.21	0.943	3.79	4.7
0.0744	0.965270	0.585	39.86	3.09	460	2.14	151	31.08	11.81	0.907	3.55	4.6
0.0923	0.970417	0.690	39.36	3.92	331	1.47	88	29.61	11.32	0.968	4.36	8.2
0.1484	0.986396	0.959	38.18	3.71	293	1.99	96	29.18	13.31	0.843	3.30	9.7
0.1810	0.995876	1.080	37.63	3.97	287	2.38	73	27.78	13.18	0.860	3.50	9.0
0.2252	1.008090	1.217	36.70	4.20	251	2.69	54	26.23	13.56	0.849	3.58	12.0
0.2715	1.020987	1.326	36.00	3.43	315	3.26	80	26.16	15.56	0.781	3.14	10.6
$\text{Sc}(\text{CF}_3\text{SO}_3)_3$												
0.0048	0.945804	0.083	37.80	0.48	264	n/a		33.27	10.50	0.983	4.05	6.9
0.0096	0.946814	0.118	38.28	1.15	307			32.86	10.41	1F <sup>c</sup>	4.27	9.7
0.0187	0.949566	0.203	39.01	2.18	301			32.99	10.78	0.961	3.84	5.1
0.0286	0.952605	0.291	39.58	3.37	296			32.66	11.32	0.922	3.55	19.2
0.0568	0.960946	0.516	39.87	4.63	239			31.78	11.65	0.899	3.46	6.5
0.0794	0.967757	0.680	39.70	5.16	211			30.89	11.68	0.910	3.65	8.1
0.1350	0.984398	1.011	38.65	5.73	172			29.33	12.42	0.879	3.59	12.3
0.1480	0.988212	1.074	38.47	5.82	167			28.81	12.17	0.901	3.84	8.6
0.1912	1.001102	1.282	37.37	5.89	145			27.59	12.77	0.883	3.89	11.0
$\text{La}(\text{CF}_3\text{SO}_3)_3$												
0.0034	0.945348	0.108	37.56	0.50	323	n/a		33.45	10.86	0.943	3.61	9.1
0.0062	0.946591	0.125	38.00	1.24	313			32.82	10.26	0.969	3.94	8.9
0.0110	0.948720	0.184	38.72	2.39	303			32.82	11.03	0.929	3.52	6.9
0.0260	0.954863	0.326	38.99	3.10	273			32.45	11.17	0.918	3.44	6.1
0.0511	0.965285	0.575	39.39	4.48	265			31.24	11.34	0.923	3.67	6.7
0.0944	0.983630	0.933	38.29	5.13	203			29.95	12.31	0.863	3.21	8.4
0.1136	0.991334	1.062	37.56	5.14	189			29.26	12.82	0.845	3.16	10.5
0.1401	1.002241	1.243	36.69	5.09	173			28.47	13.43	0.826	3.13	13.1
0.1650	1.012534	1.383	35.96	5.24	158			26.82	12.98	0.878	3.91	35.9
0.1967	1.025314	1.536	35.21	5.09	153			27.02	14.33	0.796	3.10	9.4
0.2421	1.04384	1.711	33.88	5.11	148			25.81	15.74	0.756	2.97	11.5
0.2854	1.06165	1.833	32.56	5.06	136			24.66	17.18	0.721	2.83	10.9

<sup>a</sup>Units:  $c$  in mol L<sup>-1</sup>;  $\rho$  in g cm<sup>-3</sup>;  $\kappa$  in S m<sup>-1</sup>;  $\tau_i$  in ps;  $\epsilon$ ,  $\epsilon_{\infty}$ ,  $S_p$ , and  $\beta$  are dimensionless. <sup>b</sup>The density of neat DMF varied slightly between runs and was 0.943804 g·cm<sup>3</sup> for  $\text{Sc}(\text{CF}_3\text{SO}_3)_3$  and 0.943978 g·cm<sup>3</sup> for  $\text{La}(\text{CF}_3\text{SO}_3)_3$  solutions. <sup>c</sup>Fixed value.

Table 1. This is confirmed by comparison with the spectrum of neat DMF (Figure 1).<sup>22</sup>

As discussed in detail previously,<sup>15</sup> this solvent mode is best fitted by a CD function, asymmetrically broadened at higher frequencies, to formally incorporate small contributions to the spectra from low-energy librational modes and other effects that are centered well above the present frequency range.

In addition to the dominant solvent relaxation, the present DR spectra for all three sets of salt solutions in DMF showed significant increases in amplitude at low frequencies with increasing solute concentration (Figures 1, S1, and S2 (Supporting Information)). For the  $\text{Sc}(\text{CF}_3\text{SO}_3)_3$  and  $\text{La}(\text{CF}_3\text{SO}_3)_3$  solutions, this amplitude was adequately described by a single D mode centered at ~0.4 GHz (Supporting Information Figures S3 and S4). However, for the  $\text{Al}(\text{CF}_3\text{SO}_3)_3$  solutions, two D modes, centered at ~0.5 and ~2 GHz, were required to fit the spectra (Figure 2). The various modes in the observed spectra were broadly confirmed for each salt system by Zasetsky plots.<sup>21</sup> These plots indicate (ab initio) the number of independent D processes (and their probabilities and locations) that would be required to account for the observed

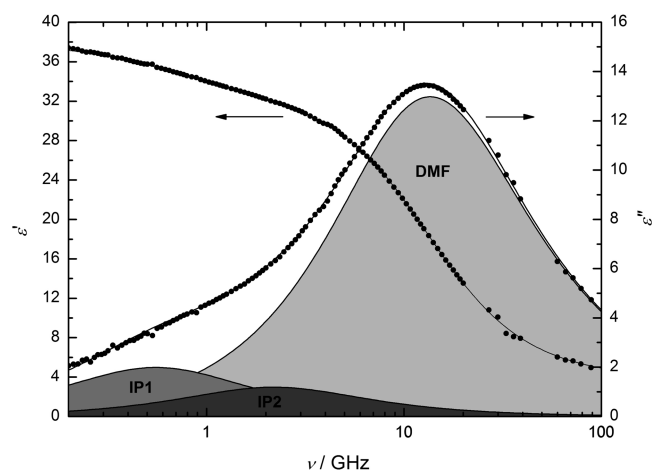


**Figure 2.** Relative permittivity,  $\epsilon'(\nu)$ , and dielectric loss,  $\epsilon''(\nu)$ , spectra of 0.1810 mol L<sup>-1</sup>  $\text{Al}(\text{CF}_3\text{SO}_3)_3$  in DMF at 25 °C. The shaded areas show the contributions of two IP species (IP1 = 2SIPs; IP2 = SIPs) and the dominant solvent relaxation process (DMF) to  $\epsilon''(\nu)$ .

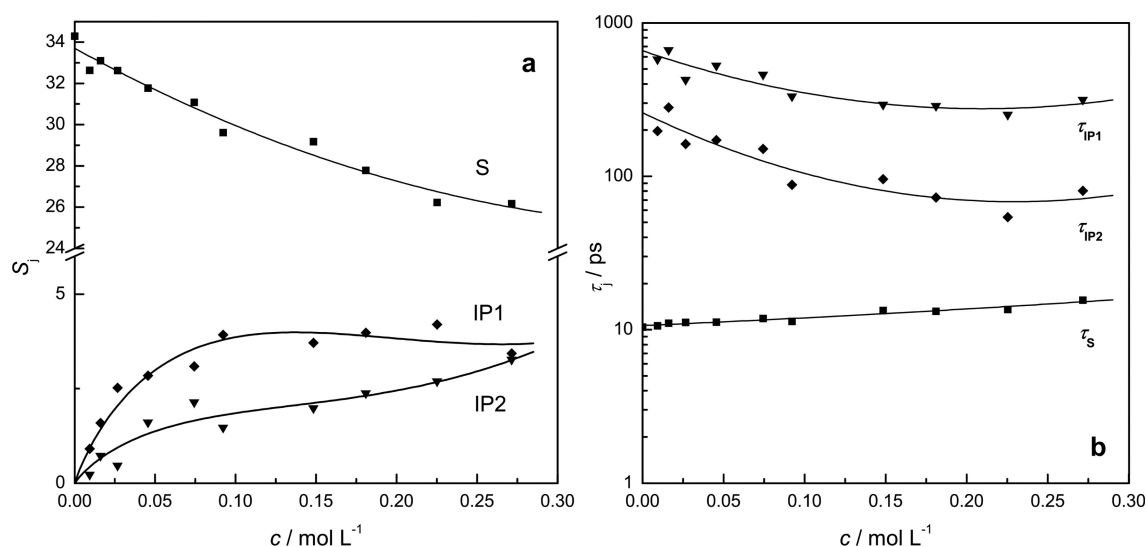


**Figure 3.** (a) Dispersion amplitudes,  $S_p$ , and (b) relaxation times,  $\tau_p$ , as functions of solute concentration,  $c$ , for solutions of  $\text{Al}(\text{CF}_3\text{SO}_3)_3$  in DMF at 25 °C. Lines are visual guides only.

spectra. As such, Zasetzky plots provide a sensible starting point for model selection, although it is emphasized (cf. section 2.3) that all plausible models were tested in the fitting process. Examples of typical Zasetzky plots, for  $\text{LaTf}_3$  in DMF, are given in the Supporting Information (Figure S5).

From the dependence of the observed amplitudes on solute concentration and their locations in the spectra, both of these lower-frequency processes (parameters  $S_{\text{IP1}}$ ,  $\tau_{\text{IP1}}$  and  $S_{\text{IP2}}$ ,  $\tau_{\text{IP2}}$ ) can be assigned to the rotational diffusion of two different types of IPs in solution (see section 3.3). The presence of appreciable ion pairing in these solutions is also indicated by the increase, above that of neat DMF, in the static permittivity,  $\epsilon$  ( $=\lim_{\nu \rightarrow 0} \epsilon'(\nu)$ ), at low solute concentrations (Figures 1, S1, and S2 (Supporting Information)) as the nonpolar cations and slightly dipolar  $\text{CF}_3\text{SO}_3^-$  anions associate to form IPs with large dipole moments. At higher  $c$ , the usual decrease in  $\epsilon$  is observed, corresponding to the significant replacement of the dipolar solvent molecules by the (less dipolar) ions and the solvation of those ions.

As just noted, the  $\text{CF}_3\text{SO}_3^-$  anions have a dipole moment ( $\mu_- \approx 3.6$  D from quantum mechanical calculations)<sup>23</sup> and therefore must contribute to the observed spectra. However, because the triflate ion is small in size ( $r_- \approx 307$  pm)<sup>11</sup> relative to any IPs (see section 3.2), the relaxation due to its rotational diffusion would be expected to occur at somewhat higher frequencies than 2 GHz. It is therefore probable that this relatively small contribution is subsumed by the broad and much more intense solvent relaxation. In the absence of a reliable theoretical method for splitting these contributions the anion contribution had to be neglected. This means that the solvation numbers calculated from the solvent relaxation (see section 3.2) are lower limits. It should also be noted that it has recently been shown that there is a small contribution to the DR spectra of all electrolyte solutions at low frequencies due to the Debye–Falkenhagen (ion cloud relaxation) effect.<sup>24</sup> Unfortunately, it is not at present possible to separate this effect theoretically, computationally, or experimentally from those arising from the presence of IPs. However, it is generally thought to be small, and in this work, it will be subsumed into the IP amplitudes.

As for other salts in DMF,<sup>14,15</sup> satisfactory fits of the spectra were therefore achieved with either a two-process (D + CD) model, for  $\text{Sc}(\text{CF}_3\text{SO}_3)_3$  and  $\text{La}(\text{CF}_3\text{SO}_3)_3$  solutions, or a three-process (D + D + CD) model, for  $\text{Al}(\text{CF}_3\text{SO}_3)_3$  solutions. The contributions of these two or three modes to typical spectra and the quality of the overall fits are illustrated in Figures 2, S3, and S4 (Supporting Information). Details of the numerical values derived from the fitting models are summarized in Table 1.

**3.2. Solvent Relaxation and Ion Solvation.** The extent of ion solvation can be determined by analyzing the solvent relaxation mode using the generalized Cavell equation,<sup>25</sup> normalized with respect to the neat solvent

$$c_j = \frac{3(\epsilon + (1 - \epsilon)A_j)}{\epsilon} \cdot \frac{k_B T \epsilon_0}{N_A} \cdot \frac{(1 - \alpha_j f_j)^2}{g_j \mu_j^2} \cdot S_j \quad (5)$$

where  $c_j$ ,  $\mu_j$ , and  $\alpha_j$  are respectively the concentration, dipole moment, and polarizability of the relaxing species,  $T$  is the thermodynamic temperature (in Kelvin),  $k_B$  and  $N_A$  are the Boltzmann and Avogadro constants, respectively, and other symbols have already been defined. The cavity-field and reaction-field factors,  $A_j$  and  $f_j$ , are defined by the size and shape of the rotating dipole,<sup>26,27</sup> while the static (Kirkwood) dipole–dipole correlation factor,  $g_j$ , accounts for orientational correlation of neighboring species of the same kind. As discussed previously,<sup>15</sup> for the present reasonably dilute solutions,  $g_{\text{DMF}}$  was assumed to be independent of the salt concentration and thus canceled out in the normalization of eq 5. This is reasonable as  $g_{\text{DMF}} \approx 1$  in neat DMF,<sup>22</sup> consistent with the absence of significant long-range dipole–dipole correlations of the solvent molecules.

The solvent dispersion amplitudes,  $S_s$  ( $=\epsilon_s - \epsilon_\infty$ ), observed for the three sets of salt solutions in DMF are listed in Table 1 and are plotted as a function of the solute concentration,  $c$ , in Figures 3, S6, and S7 (Supporting Information). Effective solvation numbers for the solute,  $Z_{\text{ib}}$ , were obtained from the  $S_s$  values, as described previously.<sup>15,19</sup> Briefly,  $S_s$  is corrected for kinetic depolarization (kd), which arises from the movement of the solvated ions in the applied field, using the Hubbard–Onsager continuum model.<sup>28,29</sup> Apparent concentrations of



rotationally free solvent molecules,  $c_s^{\text{ap}}$ , were calculated for three limiting cases: no kd and kd assuming either slip or stick boundary conditions for ion transport. Subtraction of  $c_s^{\text{ap}}$  from the analytical (total) solvent concentration,  $c_s$ , and division by the solute concentration,  $c$ , then provides an estimate of  $Z_{\text{ib}}$  as the number of irrotationally bound (ib) solvent molecules per solute “particle”

$$Z_{\text{ib}} = \frac{(c_s - c_s^{\text{ap}})}{c} \quad (6)$$

In essence,  $Z_{\text{ib}}$  is a measure of the number of solvent molecules “frozen” on the DRS time scale and, as such, is a dynamically defined quantity that is related to but not necessarily identical with a coordination number (CN).<sup>9</sup> It should also be remembered (cf. section 3.1) that because of neglect of the (small) anion contribution, the present  $Z_{\text{ib}}$  values will be underestimates, although the true values almost certainly still lie within the error bars shown in Figures 4, S8, and S9 (Supporting Information).

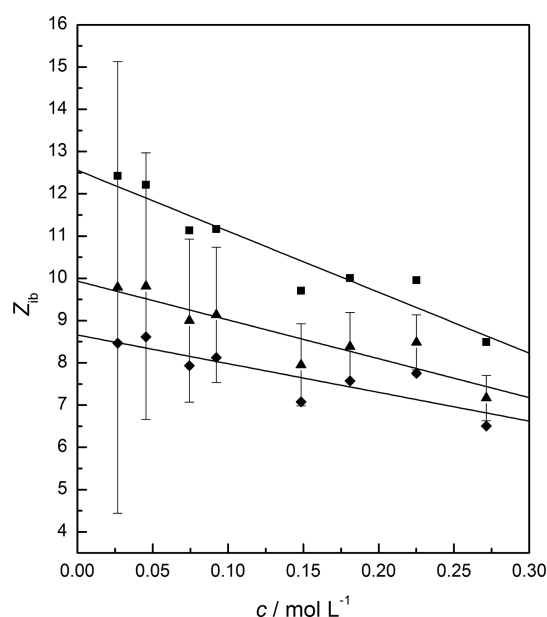


**Figure 4.** Effective solvation numbers,  $Z_{\text{ib}}$ , for  $\text{Al}(\text{CF}_3\text{SO}_3)_3$  in DMF at 25 °C as a function of solute concentration,  $c$ , under various ion-transport boundary conditions: ■ no kd, ▲ slip kd, ◆ stick kd. Error bars correspond to one standard deviation of a fit of the empirical equation  $S_s(c) = S_s(0) [34.29] + a_1c + a_2c^{3/2}$  to the experimental solvent amplitudes.

Typical results obtained for  $Z_{\text{ib}}(c)$  with  $\text{Al}(\text{CF}_3\text{SO}_3)_3$  solutions in DMF are shown in Figure 4, which also includes representative error bars. Note that the increase in the uncertainty of  $Z_{\text{ib}}(c)$  as  $c \rightarrow 0$  is normal, as discussed elsewhere.<sup>15</sup> Similar results were found for  $\text{Sc}(\text{CF}_3\text{SO}_3)_3$  and  $\text{La}(\text{CF}_3\text{SO}_3)_3$  solutions in DMF (Supporting Information, Figures S8 and S9). As is generally the case for electrolyte solutions, the values of  $Z_{\text{ib}}(c)$  depend to some extent on the assumed level of kd.<sup>9</sup> As expected, the results obtained for slip conditions, which are generally considered to be the most plausible for the translational diffusion of solvated ions, lie between those obtained assuming kd = 0 or stick conditions. Ignoring the uncertain results at low concentrations, the  $Z_{\text{ib}}(c)$  values for all three electrolytes show a reasonably smooth decrease with increasing  $c$  (Figures 4, S8, and S9 (Supporting

Information)). This decrease is observed for most electrolytes, in both aqueous and nonaqueous solutions, and is thought to reflect the effects of solvation shell overlaps.<sup>9</sup>

The infinite dilution effective solvation numbers,  $Z_{\text{ib}}^0$ , obtained for convenience by linear extrapolation of  $Z_{\text{ib}}(c)$  for each kd assumption and ignoring outliers, are collected in Table 2 and clearly indicate that all three salts are strongly solvated in

**Table 2.** Effective Solvation Numbers at Infinite Dilution,  $Z_{\text{ib}}^0$ , for  $\text{Al}(\text{CF}_3\text{SO}_3)_3$ ,  $\text{Sc}(\text{CF}_3\text{SO}_3)_3$ , and  $\text{La}(\text{CF}_3\text{SO}_3)_3$  in DMF Solutions at 25 °C Obtained Assuming Differing Ion-Transport Boundary Conditions<sup>a</sup>

electrolyte	$Z_{\text{ib}}^0$ (no kd)	$Z_{\text{ib}}^0$ (slip)	$Z_{\text{ib}}^0$ (stick)
$\text{Al}(\text{CF}_3\text{SO}_3)_3$	12.6(3)	9.9(7)	8.7(3)
$\text{Sc}(\text{CF}_3\text{SO}_3)_3$	12.5(3)	9.2(3)	8.2(2)
$\text{La}(\text{CF}_3\text{SO}_3)_3$	16.3(4)	12.6(5)	11.5(3)

<sup>a</sup>Numbers in parentheses are standard deviations in the last digit, derived from linear least-squares fits.

DMF ( $Z_{\text{ib}}^0 \gg 0$ ). As literature data indicate that the triflate ion is only weakly solvated by DMF,<sup>11,14</sup> it is reasonable to assume that  $Z_{\text{ib}}^0(\text{CF}_3\text{SO}_3^-) \approx 0$  and thus to assign all of the ib DMF molecules to the cations.<sup>15</sup> Taking the  $Z_{\text{ib}}^0$  values calculated under slip conditions (Table 2) as the best estimates, it can be concluded that the present DR spectra indicate ( $Z_{\text{ib}}^0(\text{Al}^{3+}) \approx Z_{\text{ib}}^0(\text{Sc}^{3+}) \approx 10$ ) < ( $Z_{\text{ib}}^0(\text{La}^{3+}) \approx 13$ ). These  $Z_{\text{ib}}^0$  values are broadly consistent with those obtained previously by DRS for monovalent and divalent cations in DMF,<sup>14,15</sup> however, as would be expected from their higher charge, the present values for  $\text{M}^{3+}$  are significantly larger.

The strong solvation of these cations by DMF might, at first glance, appear surprising but is consistent with the strong donor properties of DMF.<sup>1</sup> Values of the Gibbs energies of solvation,  $\Delta_{\text{solv}}G^\circ$ , corresponding to the process  $\text{M}^{n+}(\text{g}) + \infty\text{DMF} \rightarrow \text{M}^{n+}(\text{solv})^2$  have not been reported for these ions but can be readily calculated using an appropriate thermodynamic cycle<sup>30</sup> as the sum of their hydration and transfer ( $\text{H}_2\text{O} \rightarrow \text{DMF}$ ) energies,  $\Delta_{\text{hyd}}G^\circ + \Delta_{\text{t}}G^\circ$ . The latter are also not known for  $\text{M}^{3+}$  ions but can be estimated by comparison with the established values for other polyvalent cations,<sup>5</sup> to be  $\sim -50$  kJ mol<sup>-1</sup>. This is negligible in comparison with the hydration energies, and thus,  $\Delta_{\text{solv}}G^\circ(\text{M}^{3+}, \text{DMF}) \approx \Delta_{\text{hyd}}G^\circ(\text{M}^{3+}, \text{aq}) \approx -4500$  ( $\text{Al}^{3+}$ ),  $-3800$  ( $\text{Sc}^{3+}$ ), and  $-3200$  ( $\text{La}^{3+}$ ) kJ mol<sup>-1</sup>.

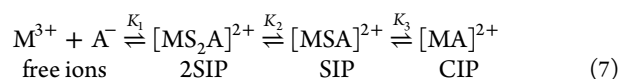
It is interesting to compare the  $Z_{\text{ib}}^0$  values of these cations in DMF with the CNs (average number of nearest neighbors) obtained experimentally using XRD, EXAFS, and so forth or by computer simulations. As in water and other solvents,  $\text{Al}^{3+}$  has a CN of strictly 6 in DMF.<sup>31</sup> This is certainly a reflection of the steric requirements for packing relatively bulky solvent molecules around the very small  $\text{Al}^{3+}$  ion ( $r_+ = 53$  pm; all radii are from Marcus<sup>11</sup>). The  $\text{Sc}^{3+}$  ion ( $r_+ = 75$  pm) does not appear to have been studied in DMF, but although its CN in other solvents (including water) is often controversial, it should have a CN of  $\sim 6$  or slightly higher.<sup>32</sup> The CN of the much larger  $\text{La}^{3+}$  ( $r_+ = 105$  pm) is also often controversial; in DMF, values of between 7 and 9 have been reported, with the latter being more common.<sup>33,34</sup> The CNs for all three of these cations are significantly less than the present  $Z_{\text{ib}}^0$  values (even with stick boundary conditions for kd; Table 2). This means that in DMF, all of the present cations must have a significant second solvation shell in which the solvent molecules are sufficiently tightly bound so as to be immobilized on the DRS

time scale. It is reasonable to assume that the CNs correspond to the number of ib DMF molecules in the first (inner) solvation shell, that is,  $Z_{ib,1}^0 \approx \text{CN} \approx 6$  ( $\text{Al}^{3+}$ ,  $\text{Sc}^{3+}$ ) or  $\approx 9$  ( $\text{La}^{3+}$ ). It therefore follows that the number of ib DMF molecules in the second (outer) solvation shell is roughly constant,  $Z_{ib,2}^0 = Z_{ib}^0 - Z_{ib,1}^0 \approx 4$ , for all three cations. Note that this does not necessarily mean that four DMF molecules residing in the second shell are completely immobilized but rather that there are enough DMF molecules whose motion is sufficiently restricted such that the “lost” total dipole moment sums to  $4\mu_{\text{DMF}}$ .

This unexpected constancy of  $Z_{ib,2}^0$  probably reflects an attenuation of the differences (especially with respect to size and hence charge/radius ratio) among the bare cations by the inner solvation shell of DMF molecules. A similar effect is indeed apparent for the two divalent cations studied previously.<sup>15</sup> Under slip conditions,  $Z_{ib}^0$  values were found to be  $\sim 8.5$  and  $\sim 10.6$  for  $\text{Mg}^{2+}$  and  $\text{Ba}^{2+}$ , respectively. The CNs of these two ions in DMF have been estimated to be  $\sim 6$  for  $\text{Mg}^{2+}$  ( $r_+ = 75$  pm) from XRD (in the solid state)<sup>35</sup> and Raman spectroscopy (in solution)<sup>36</sup> and  $\sim 8$  for  $\text{Ba}^{2+}$  ( $r_+ = 136$  pm), also by Raman.<sup>36</sup> Again, assuming that  $Z_{ib,1}^0 \approx \text{CN}$  for the cations gives an approximately constant value of  $Z_{ib,2}^0 \approx 2.5$  for these two divalent cations, which is consistent with their lower charge/radius ratios compared to those for the present  $\text{M}^{3+}$  ions.

As noted previously,<sup>15</sup> the solvation of monovalent and divalent cations in DMF is very different from that in water;<sup>37,38</sup> the same is true for the present trivalent cations. Approximate  $Z_{ib}^0$  values for  $\text{Al}^{3+}$ ,  $\text{Sc}^{3+}$ , and  $\text{La}^{3+}$  in aqueous solution of 30,<sup>20</sup> 18,<sup>39</sup> and 16,<sup>40</sup> respectively, have been reported from DRS measurements. Given that the corresponding CNs of these ions in water are typically 6, 6+, and 9, respectively, this indicates extensive ( $Z_{ib,2}^0(\text{La}^{3+}) \approx 7$ ;  $Z_{ib,2}^0(\text{Sc}^{3+}) \approx 12$ ) or even complete ( $Z_{ib,2}^0(\text{Al}^{3+}) > 18$ ) formation of a second hydration shell. Indeed, if the  $Z_{ib}^0$  values are taken at face value, as noted previously,<sup>20</sup> there appears to be a partial formation of a third hydration shell around  $\text{Al}^{3+}$  ( $Z_{ib,3}^0 = Z_{ib}^0 - Z_{ib,1}^0 - Z_{ib,2}^0 \approx 30 - 6 - 12 \approx 12$ ), which is highly unusual. The differences between the solvation of these ions in water and DMF are largely a reflection of the extent and strength of H-bonding in the former, its higher dielectric constant, and the smaller steric requirements of water molecules.<sup>13</sup>

**3.3. Solute Relaxations and Ion Association.** Because of the strong Coulombic attraction between ions in solution, ion association is always present to some extent in electrolyte solutions. This is especially true in solvents such as DMF that have a lower dielectric constant (relative permittivity) than water ( $\epsilon_{\text{DMF}} = 36.71$  at  $25^\circ\text{C}$ )<sup>12</sup> because higher solvent permittivity stabilizes the free ions relative to their lower-charged associates.<sup>41</sup> Ion association in salt solutions is well described by the Eigen–Tamm model,<sup>9,42</sup> which posits that solvated ions initially combine with their (inner) solvation shells essentially intact to form double-solvent-separated ion pairs (2SIPs). These 2SIPs can then lose the intervening solvent molecules to form solvent-shared (SIPs) and finally contact ion pairs (CIPs). Assuming that only IPs of 1:1 stoichiometry are formed, this process can be represented for the present 3:1 electrolytes as



where all species are assumed to be solvated to a greater (the free ions) or lesser (the partially charge-neutralized IPs) extent. Note that this solvation is in addition to the specified solvent molecules (S) located between the charge centers (cf. eq 7). While the Eigen–Tamm model provides a general description of ion association in solution, this does not necessarily mean that all species form to a significant extent (ie, are detectable) in any particular system.<sup>43</sup>

**IP Relaxation Times.** The DR spectra of each of the present 3:1 electrolytes in DMF exhibited increases in intensity (amplitude) at low frequencies with increasing solute concentration (Figures 1, S1, and S2 (Supporting Information)). These increases can be assigned (section 3.1) to the presence of one or two IP types. To help determine which types of IP are present, the observed relaxation times can be compared with theoretically derived values. To make this comparison, the observed (macroscopic) relaxation time  $\tau_{\text{obs}}$  must be converted to the required “molecular” rotational correlation time  $\tau'_{\text{obs}}$ . For a D mode, this can be done via the Powles–Glarum equation<sup>44,45</sup>

$$\tau'_{\text{obs}} = \frac{2\epsilon + \epsilon_{\infty}}{3\epsilon} \cdot \tau_{\text{obs}} \quad (8)$$

where  $\epsilon_{\infty}$  is here the high-frequency limit of the solute relaxation.

The  $\tau'_{\text{obs}}$  so obtained can then be compared with the corresponding rotational correlation times  $\tau'$  calculated via the Stokes–Einstein–Debye (SED) equation<sup>46,47</sup>

$$\tau' = \frac{3V_r}{k_B} \cdot \frac{\eta}{T} \quad (9)$$

where  $V_r$  is the (molecular) volume of rotation of the relaxing species,  $\eta$  is the bulk solution viscosity, and the other symbols have already been defined. The rotation volume is calculated as  $V_r = V_m f_{\perp} C$ , where  $V_m$  is the actual geometric volume of the rotating species,  $f_{\perp}$  is a shape factor, and  $C$  is the hydrodynamic coupling constant between the rotating species and its environment ( $C = 1$  for stick or  $C = 1 - f_{\perp}^{-2/3}$  for slip boundary conditions). For simplicity, IPs were approximated as prolate ellipsoids, as described previously,<sup>15</sup> and in the absence of experimental data, solution viscosities were assumed to be the same as that for neat DMF ( $\eta = 802 \mu\text{Pa s}$  at  $25^\circ\text{C}$ ).<sup>12</sup> Note that the calculation of  $V_m f_{\perp}$  refers to bare IPs. Slip conditions should apply for rotation of an unsolvated IP, whereas stick conditions are compatible with strong solvation. For the present salts, consisting of strongly solvated cations but only weakly solvated anions, a  $C$  value closer to stick can be expected, within the limits of the SED model, originally derived for a macroscopic body rotating in a structureless medium.

Molecular relaxation times calculated via eq 9 for all three IP types rotating under both slip and stick conditions are summarized in Table 3, along with the observed values. Unfortunately, as found previously for 1:1 and 2:1 electrolytes in DMF,<sup>15</sup> the  $\tau'$  values calculated via the SED model do not unequivocally identify the IP type. Nevertheless, on the basis of the strong solvation of the cations and the weak solvation of the anions, SIPs are most plausible for the two salts (Sc and La triflate) that show only one solute-related process. For  $\text{AlTf}_3$  solutions, which exhibit two solute-related processes, the slowest (IP1) process almost certainly arises from the rotational diffusion of 2SIPs and IP2 from SIPs.

**Table 3.** Comparison of Experimental,  $\tau'_{\text{obs}}$ ,<sup>a</sup> and Calculated Rotational Correlation Times for Stick and Slip Boundary Conditions,  $\tau'_{\text{stick}}$  and  $\tau'_{\text{slip}}$ ,<sup>b</sup> for IP Reorientation in  $\text{MTf}_3$  Solutions in DMF at 25 °C<sup>c</sup>

electrolyte	$\tau'_{\text{obs}}$	IP	$\tau'_{\text{slip}}$	$\tau'_{\text{stick}}$
$\text{Al}(\text{CF}_3\text{SO}_3)_3$	199 ( $\tau_2$ ), 540 ( $\tau_1$ )	CIP	16	220
		SIP	66	353
		2SIP	155	537
$\text{Sc}(\text{CF}_3\text{SO}_3)_3$	294	CIP	18	254
		SIP	70	399
		2SIP	164	596
$\text{La}(\text{CF}_3\text{SO}_3)_3$	291	CIP	19	306
		SIP	76	467
		2SIP	175	684

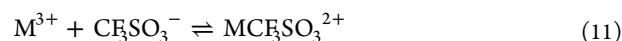
<sup>a</sup>Obtained via the Powles–Glarum relation (eq 8). <sup>b</sup>Obtained from the SED relation (eq 9). <sup>c</sup>Unit: all  $\tau$  values in ps.

**Association Constants.** The Cavell equation (eq 5) can be used to estimate the IP concentrations,  $c_{\text{IP}}$ , from the observed solute-related amplitudes (collectively labeled  $S_{\text{IP}}$ ). The required input parameters for eq 5,  $\alpha_{\text{IP}}$ ,  $g_{\text{IP}}$ ,  $A_{\text{IP}}$ ,  $f_{\text{IP}}$ , and  $\mu_{\text{IP}}$ , were calculated for all IP types, but only the results for the most plausible structures (section 3.1) will be discussed here; an extended account of these calculations is given elsewhere.<sup>15</sup> IP polarizabilities were estimated as  $\alpha_{\text{IP}} = \alpha_+ + \alpha_- + n\alpha_{\text{DMF}}$ , where  $\alpha/4\pi\epsilon_0 \text{ \AA}^3 = 0.0393$  ( $\text{Al}^{3+}$ ),<sup>48</sup> 0.634 ( $\text{Sc}^{3+}$ ),<sup>11</sup> 1.086 ( $\text{La}^{3+}$ ),<sup>11</sup> 6.84 ( $\text{CF}_3\text{SO}_3^-$ ), and 7.88 (DMF),<sup>22</sup> with  $n = 0, 1$  or  $2$ , corresponding to CIPs, SIPs and 2SIPs, respectively. The value of  $g_{\text{IP}}$  was taken to be unity throughout because IP concentrations are sufficiently low so that interactions between them should be negligible. The field factors  $A_{\text{IP}}$  and  $f_{\text{IP}}$  were calculated geometrically using standard procedures.<sup>25</sup> Dipole moments in solution,  $\mu_{\text{IP}}$ , were calculated as described previously.<sup>15</sup> This involves allowing for the presence of  $n$  oriented DMF molecules between the charge centers, the effects of ion polarizability, and the permanent dipole of  $\text{Tf}^-$ . Note too that for the present asymmetric electrolytes, the 1:1 IPs carry a net positive charge and thus no longer have a uniquely defined reference point for calculating their dipole moments. As previously,<sup>15,20</sup> the center of hydrodynamic stress, rather than the center of mass, was taken as the pivot for this purpose. Ionic radii (of the bare ions in pm from Marcus<sup>11</sup> unless otherwise specified) assumed for the dipole moment calculations were 53 ( $\text{Al}^{3+}$ ), 75 ( $\text{Sc}^{3+}$ ), 105 ( $\text{La}^{3+}$ ), 307 ( $\text{CF}_3\text{SO}_3^-$ , taken as an ellipsoid),<sup>49</sup> and 330 (DMF).<sup>14</sup> All other details are as described previously.<sup>15</sup>

Assuming that only IPs of 1:1 stoichiometry are formed, the overall ion association constant,  $K_{\text{A}}$ , is given by

$$K_{\text{A}} = \frac{c_{\text{IP}}}{c_+ c_-} \quad (10)$$

and corresponds to the equilibrium (with all species solvated)



where  $c_{\text{IP}}$  is the total IP concentration (i.e., the sum of the concentrations of all of the 1:1 IP types present in solution) and  $c_+$  and  $c_-$  are free cation and anion concentrations, respectively. Using  $c_{\text{IP}}$  values calculated via eq 5 and the appropriate mass balance relationships yields  $K_{\text{A}}(c)$  values at each salt concentration. These values were then fitted for convenience with an extended form of the Guggenheim equation<sup>50</sup>

$$\log K_{\text{A}} = \log K_{\text{A}}^\circ - \frac{2A_{\text{DH}}|z_+ z_-| \sqrt{I}}{1 + A_{\text{K}} \sqrt{I}} + B_{\text{K}} I + C_{\text{K}} I^{3/2} \quad (12)$$

to provide the standard state (infinite dilution) constant,  $K_{\text{A}}^\circ$ , where  $A_{\text{DH}}$  is the Debye–Hückel constant for DMF ( $=1.5554 \text{ L}^{1/2} \text{ mol}^{-1/2}$  at 25 °C),  $Y_{\text{K}}$  ( $Y = \text{A}, \text{B}, \text{C}$ ) are fitting parameters, and  $I (=0.5 \sum c_i z_i^2)$  is the stoichiometric ionic strength. The values of  $K_{\text{A}}(c)$  and hence of  $K_{\text{A}}^\circ$  depend on the structures of the IPs assumed to be present;<sup>15,20</sup> consequently, the following discussion is restricted to the most probable IP types.

While parameter correlations precluded reliable estimation of  $K_{\text{A}}^\circ(\text{LaTf}^{2+})$ , values of  $K_{\text{A}}^\circ/\text{L mol}^{-1} = 1000 \pm 30$  and  $370 \pm 20$  were obtained for  $\text{AlTf}^{2+}$  and  $\text{ScTf}^{2+}$ , respectively, assuming the presence of 2SIPs and SIPs for the former and SIPs for the latter (section 3.1). These two  $K_{\text{A}}^\circ$  results are broadly consistent with the values of  $K_{\text{A}}^\circ(\text{MgTf}^+) = 84 \pm 7$  and  $K_{\text{A}}^\circ(\text{NaTf}^0) = 5 \pm 2$  obtained previously by DRS and suggest an essentially electrostatic interaction between the strongly solvated cations and the triflate anion.<sup>41</sup>

It would be interesting to compare the present  $K_{\text{A}}^\circ$  results with those obtained by reliable conventional techniques such as conductometry. Unfortunately, according to a recent comprehensive review of conductivity studies in nonaqueous solutions,<sup>7</sup> few reliable data are available for 3:1 electrolytes in DMF. Reanalysis of the available data (for  $\text{Al}(\text{ClO}_4)_3$  and  $\text{In}(\text{ClO}_4)_3$ ) using a well-established theoretical model produced no evidence of ion association.<sup>7</sup> This seems highly unlikely given that the same analysis<sup>7</sup> suggested  $K_{\text{A}}^\circ$  values of (10–30)  $\text{L mol}^{-1}$  for a variety of  $\text{M}(\text{ClO}_4)_2$  solutions in DMF, consistent with our previous DRS finding of  $K_{\text{A}}^\circ(\text{BaClO}_4^+) = 21 \pm 6 \text{ L mol}^{-1}$  in this solvent.<sup>15</sup> Association constants of this magnitude should be easily detectable by electrical conductivity measurements.<sup>41</sup> This underlines the very real experimental difficulties involved in making measurements of even modest accuracy in nonaqueous solutions even when using well-established and straightforward techniques such as conductometry.

The  $K_{\text{A}}$  values for the present 3:1 electrolytes in DMF indicate significant levels of ion pairing. However, as would be expected from the large Debye–Hückel effect for such highly charged ions<sup>50</sup> (the numerator in the second term on the right-hand side of eq 12), they decrease very quickly with increasing solute concentration. This effect is illustrated for  $\text{AlTf}_3$  solutions in Figure 5, which shows  $K_{\text{A}}(\text{AlTf}^{2+}) < 1 \text{ L mol}^{-1}$  at  $I \gtrsim 1$  (i.e.,  $c \gtrsim 0.17 \text{ mol L}^{-1}$ ). The dramatic decrease in  $K_{\text{A}}$  with increasing  $I$  produces the well-known “redissociation” effect, which causes electrolytes to be much less associated at high concentrations than would be expected. Figure 5 also shows that the values of  $K_{\text{A}} (=K_1 + K_1 K_2)$  closely parallel those of  $K_1$ , as would be expected from the nature of the species involved (cf. eq 7), while  $K_2$ , which involves only a loss of solvent, is almost independent of  $I$ .

#### 4. CONCLUDING REMARKS

The present dielectric spectroscopy measurements of  $\text{MTf}_3$  ( $\text{M} = \text{Al}, \text{Sc}, \text{La}$ ) in DMF solutions, the first on 3:1 electrolytes in any solvent other than water, have shown that the cations are very highly solvated with effective solvation numbers ( $Z_{\text{ib}}$  values) of at least 10 DMF molecules, indicative of the (partial) formation of a second solvation shell around each cation. Because of this high level of solvation, which leads to the formation of solvent-separated ion pairs (SIPs and 2SIPs), coupled with a large Debye–Hückel effect due to their high



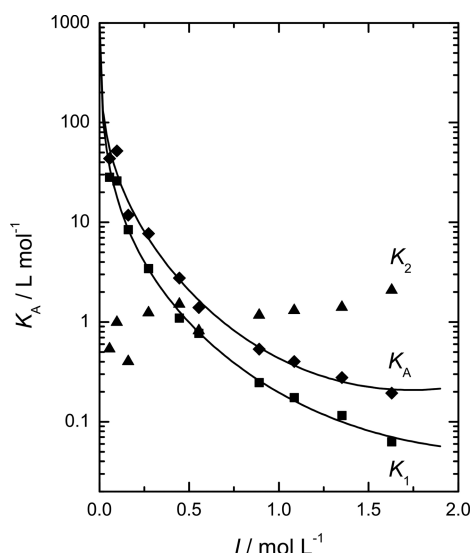


**Figure 5.** Overall association constant,  $K_A$ , and stepwise formation constants,  $K_1$  and  $K_2$ , for 1:1 IPs in DMF solutions of  $\text{Al}(\text{CF}_3\text{SO}_3)_3$  at 25 °C as functions of ionic strength,  $I$ , assuming a 2SIP + SIP speciation model. Curves for  $K_A$  and  $K_1$  are fits using eq 12 with the  $Y_K$  parameters listed in the Supporting Information, Table S1.

cationic charge, these 3:1 salts are much less associated in DMF than might be expected given the modest dielectric constant of the solvent.

## ■ ASSOCIATED CONTENT

### ■ Supporting Information

A table with the empirical parameters of eq 12 for  $K_A^\circ(\text{MTf}^{2+})$ ,  $M = \text{Al}$  or  $\text{Sc}$ , figures analogous to Figures 1–4 for  $\text{ScTf}_3$  and  $\text{LaTf}_3$  in DMF, and two representative Zaslavsky plots. This material is available free of charge via the Internet at <http://pubs.acs.org>.

## ■ AUTHOR INFORMATION

### Corresponding Authors

\*E-mail: [g.hefter@murdoch.edu.au](mailto:g.hefter@murdoch.edu.au) (G.H.).

\*E-mail: [richard.buchner@chemie.uni-regensburg.de](mailto:richard.buchner@chemie.uni-regensburg.de) (R.B.).

### Notes

The authors declare no competing financial interest.

\*A.F.: née Placzek.

## ■ ACKNOWLEDGMENTS

A.F.'s stays in Australia and Germany were funded by Murdoch University and the German Academic Exchange Service (DAAD), respectively.

## ■ REFERENCES

- (1) Marcus, Y. *Ion Solvation*; Wiley: New York, 1985.
- (2) Popovych, O.; Tomkins, R. P. T. *Nonaqueous Solution Chemistry*; Wiley-Interscience: New York, 1981.
- (3) Plechkova, N. V.; Rogers, R. D.; Seddon, K. R., Eds.; *Ionic Liquids: From Knowledge to Application*; ACS Symposium Series; American Chemical Society: Washington, DC, 2009; Vol. 1030.
- (4) Marcus, Y.; Hefter, G. Standard Partial Molar Volumes of Electrolytes and Ions in Nonaqueous Solvents. *Chem. Rev.* **2004**, *104*, 3405–3452.
- (5) Kalidas, C.; Hefter, G.; Marcus, Y. Gibbs Energies of Transfer of Cations from Water to Mixed Aqueous Organic Solvents. *Chem. Rev.* **2000**, *100*, 819–852.

(6) Jenkins, H. D. B.; Marcus, Y. Ionic B-Coefficients in Solution. *Chem. Rev.* **1995**, *95*, 2695–2726.

(7) Apelblat, A. Representation of Electrical Conductances for Polyvalent Electrolytes by the Quint-Viallard Conductivity Equation. Part 4. Symmetrical 2:2, 3:3 and Unsymmetrical 2:1, 3:1 and 1:3 Type Electrolytes in Pure Organic Solvents. *J. Solution Chem.* **2011**, *40*, 1234–1257, and references cited therein.

(8) Buchner, R. In *Novel Approaches to the Structure and Dynamics of Liquids: Experiments, Theories and Simulations*; Samios, J., Durov, V. A., Eds.; Kluwer: Dordrecht, The Netherlands, 2004.

(9) Buchner, R.; Hefter, G. Interactions and Dynamics in Electrolyte Solutions by Dielectric Spectroscopy. *Phys. Chem. Chem. Phys.* **2009**, *11*, 8984–8999.

(10) Barthel, J.; Buchner, R.; Münsterer, M. In *Electrolyte Data Collection, Part 2: Dielectric Properties of Water and Aqueous Electrolyte Solutions*; Chemistry Data Series; Kreysa, G., Ed.; DECHEMA: Frankfurt, Germany, 1995; Vol. XII.

(11) Marcus, Y. *Ion Properties*; Dekker: New York, 1997.

(12) Marcus, Y. *The Properties of Solvents*; Wiley: London, 1998.

(13) Placzek, A.; Grzybowski, W.; Hefter, G. Molar Volumes and Heat Capacities of Electrolytes and Ions in *N,N*-Dimethylformamide. *J. Phys. Chem. B* **2008**, *112*, 12366–12373.

(14) Wurm, B.; Münsterer, M.; Richardi, J.; Buchner, R.; Barthel, J. Ion Association and Solvation of Perchlorate Salts in *N,N*-Dimethylformamide and *N,N*-Dimethylacetamide. A Dielectric Relaxation Study. *J. Mol. Liq.* **2005**, *119*, 97–106.

(15) Placzek, A.; Hefter, G. T.; Rahman, H. M. A.; Buchner, R. Dielectric Relaxation Study of the Ion Solvation and Association of  $\text{NaCF}_3\text{SO}_3$ ,  $\text{Mg}(\text{CF}_3\text{SO}_3)_2$ , and  $\text{Ba}(\text{ClO}_4)_2$  in *N,N*-Dimethylformamide. *J. Phys. Chem. B* **2011**, *115*, 2234–2242.

(16) Chadwick, S. S. *Ullmann's Encyclopedia of Industrial Chemistry*; Wiley-VCH: Weinheim, Germany, 2006.

(17) Buchner, R.; Hefter, G. T.; May, P. M. Dielectric Relaxation of Aqueous NaCl Solutions. *J. Phys. Chem. A* **1999**, *103*, 1–9.

(18) Barthel, J.; Buchner, R.; Eberspächer, P. N.; Münsterer, M.; Stauber, J.; Wurm, B. Dielectric Relaxation of Electrolyte Solutions. Recent Developments and Prospects. *J. Mol. Liq.* **1998**, *78*, 82–109.

(19) Buchner, R.; Chen, T.; Hefter, G. Complexity in 'Simple' Electrolyte Solutions: Ion Pairing in  $\text{MgSO}_4(\text{aq})$ . *J. Phys. Chem. B* **2004**, *108*, 2365–2375.

(20) Schrödle, S.; Rudolph, W. W.; Hefter, G. T.; Buchner, R. Ion Association and Hydration in 3:2 Electrolyte Solutions by Dielectric Spectroscopy: Aluminium Sulfate. *Geochim. Cosmochim. Acta* **2007**, *71*, 5287–5300.

(21) Zaslavsky, A. Y.; Buchner, R. Quasi-linear Least Squares and Computer Code for Numerical Evaluation of Relaxation Time Distribution from Broadband Dielectric Spectra. *J. Phys.: Condens. Matter* **2011**, *23*, 025903.

(22) Barthel, J.; Buchner, R.; Wurm, B. The Dynamics of Liquid Formamide, *N*-Methylformamide, *N,N*-Dimethylformamide, and *N,N*-Dimethylacetamide. A Dielectric Relaxation Study. *J. Mol. Liq.* **2002**, *98–99*, 51–69.

(23) Stewart, J. J. P. *MOPAC2009*, version 9.097W; Stewart Computational Chemistry: Colorado Springs, CO, 2009.

(24) Yamaguchi, T.; Matsuoka, T.; Koda, S. A Theoretical Study on the Frequency-Dependent Electric Conductivity of Electrolyte Solutions. II. Effect of Hydrodynamic Interaction. *J. Chem. Phys.* **2009**, *130*, 094506.

(25) Barthel, J.; Hetzenauer, H.; Buchner, R. Dielectric Relaxation of Aqueous Electrolyte Solutions. II. Ion-Pair Relaxation of 1:2, 2:1, and 2:2 Electrolytes. *Ber. Bunsen-Ges. Phys. Chem.* **1992**, *96*, 1424–1432.

(26) Böttcher, C. F. J. *Theory of Electric Polarization*, 2nd ed.; Elsevier: Amsterdam, The Netherlands, 1973; Vol. 1.

(27) Böttcher, C. F. J.; Bordewijk, P. *Theory of Electric Polarization*, 2nd ed.; Elsevier: Amsterdam, The Netherlands, 1978; Vol. 2.

(28) Hubbard, J.; Onsager, L. Dielectric Dispersion and Dielectric Friction in Electrolyte Solutions. I. *J. Chem. Phys.* **1977**, *67*, 4850–4857.



- (29) Hubbard, J. B. Dielectric Dispersion and Dielectric Friction in Electrolyte Solutions. II. *J. Chem. Phys.* **1978**, *68*, 1649–1664.
- (30) Hefter, G. T. Ion Solvation in Aqueous–Organic Mixtures. *Pure Appl. Chem.* **2005**, *77*, 605–617.
- (31) Suzuki, H.; Ishiguro, S.-I. *N,N*-Dimethylformamide Complex of Aluminium(III) Perchlorate. *Acta Crystallogr., Sect. C* **1998**, *54*, 586–588.
- (32) Cotton, S. A. Recent Advances in the Chemistry of Scandium. *Polyhedron* **1999**, *18*, 1691–1715.
- (33) Ishiguro, S.-I.; Umebayashi, Y.; Kato, K.; Takahashi, R.; Ozutsumi, K. Strong and Weak Solvation Steric Effects on Lanthanoid(III) Ions in *N,N*-Dimethylformamide–*N,N*-Dimethylacetamide Mixtures. *J. Chem. Soc., Faraday Trans.* **1998**, *94*, 3607–3612.
- (34) See, for example: Berthet, J.-C.; Theury, P.; Ephritikhine, M. First Characterization of an Uranium(III) Complex with a Carbonyl-Containing Ligand: Syntheses and X-ray Crystal Structures of the Homoleptic Dimethylformamide Complexes  $(M(\text{dmf})_n)_3$  ( $M = \text{Ce}$ ,  $\text{Nd}$  and  $n = 8$ ;  $M = \text{La}$ ,  $\text{Ce}$ ,  $\text{U}$  and  $n = 9$ ). *Polyhedron* **2006**, *25*, 1700–1706.
- (35) Rao, C. P.; Rao, A. M.; Rao, C. N. R. Crystal and Molecular Structures of Alkali- and Alkaline-Earth-Metal Complexes of *N,N*-Dimethylformamide. *Inorg. Chem.* **1984**, *23*, 2080–2085.
- (36) Asada, M.; Fujimori, T.; Fujii, K.; Kanzaki, R.; Umebayashi, Y.; Ishiguro, S.-I. Solvation Structure of Magnesium, Zinc, and Alkaline Earth Metal Ions in *N,N*-Dimethylformamide, *N,N*-Dimethylacetamide, and Their Mixtures Studied by Means of Raman Spectroscopy and DFT Calculations—Ionic Size and Electronic Effects on Steric Congestion. *J. Raman Spectrosc.* **2007**, *38*, 417–426.
- (37) Ohtaki, H.; Radnai, T. Structure and Dynamics of Hydrated Ions. *Chem. Rev.* **1993**, *93*, 1157–1204.
- (38) Marcus, Y. Effect of Ions on the Structure of Water: Structure Making and Breaking. *Chem. Rev.* **2009**, *109*, 1346–1370.
- (39) Schrödle, S.; Wachter, W.; Buchner, R.; Hefter, G. T. Scandium Sulfate Complexation in Aqueous Solution by Dielectric Relaxation Spectroscopy. *Inorg. Chem.* **2008**, *47*, 8619–8628.
- (40) Buchner, R.; Barthel, J.; Gill, B.  $\text{La}(\text{Fe}(\text{CN})_6)_3$  Ion Pairing in Aqueous Solutions. A Dielectric Relaxation Study. *Phys. Chem. Chem. Phys.* **1999**, *1*, 105–109, assuming  $Z_{\text{ib}}^0((\text{Fe}(\text{CN})_6)^{3-}) \approx 0$  and slip kd..
- (41) Marcus, Y.; Hefter, G. Ion Pairing. *Chem. Rev.* **2006**, *106*, 4585–4621.
- (42) Eigen, M.; Tamm, K. Schallabsorption in Elektrolytlösungen als Folge Chemischer Relaxation II. Meßergebnisse und Relaxationsmechanismen für 2–2-Wertige Elektrolyte. *Z. Elektrochem.* **1962**, *66*, 107–121.
- (43) Hefter, G. T. When Spectroscopy Fails: The Measurement of Ion Pairing. *Pure Appl. Chem.* **2006**, *78*, 1571–1586.
- (44) Powles, J. G. Dielectric Relaxation and the Internal Field. *J. Chem. Phys.* **1953**, *21*, 633–637.
- (45) Glarum, S. H. Dielectric Relaxation of Isoamyl Bromide. *J. Chem. Phys.* **1960**, *33*, 639–643.
- (46) Dote, J. L.; Kivelson, D. Hydrodynamic Rotational Friction Coefficients for Nonspheroidal Particles. *J. Phys. Chem.* **1983**, *87*, 3889–3893.
- (47) Alavi, D. S.; Hartman, R. S.; Waldeck, D. H. A Test of Continuum Models for Dielectric Friction. Rotational Diffusion of Phenoxazine Dyes in Dimethylsulfoxide. *J. Chem. Phys.* **1991**, *94*, 4509–4520.
- (48) Pyper, N. C.; Pike, C. G.; Edwards, P. P. The Polarizabilities of Species Present in Ionic Solutions. *Mol. Phys.* **1992**, *76*, 353–372.
- (49) Okan, S. E.; Champeney, D. C. Molar Conductance of Aqueous Solutions of Sodium, Potassium, and Nickel Trifluoromethanesulfonate at 25°C. *J. Solution Chem.* **1997**, *26*, 405–414.
- (50) Robinson, R. A.; Stokes, R. H. *Electrolyte Solutions*, 2nd ed.; Butterworths: London, 1970.